



ELSEVIER

Invited paper

Perspectives in element-specific magnetic domain imaging

C.M. Schneider *

Max-Planck-Institut für Mikrostrukturphysik, Am Weinberg 2, D-06120 Halle / Saale, Germany

Abstract

The discovery of magnetic dichroism in high-energy spectroscopies has opened up new opportunities for the spatially resolved investigation of magnetic microstructures. Involving characteristic electronic levels of the solid, soft X-ray magneto-dichroic effects combine magnetic sensitivity with elemental selectivity and thus permit element-specific analyses of magnetic phenomena. Of particular interest is their use as a contrast mechanism in magnetic domain imaging.

1. Introduction

The magnetism of thin films is currently receiving wide interest from both basic research and technology. This interest is nourished by a number of fascinating effects which have been observed in thin film systems, such as an oscillatory interlayer exchange coupling in sandwich structures [1–3], or the giant magnetoresistance (GMR) in multilayers [4,5]. Understanding the underlying physical mechanisms of these phenomena remains a considerable task in the field of basic research. At the same time, significant improvements in the capacity and performance of storage devices may be expected by the introduction and consequent exploitation of these new effects in magnetic recording technology. From the viewpoint of materials research, the optimization of particular magnetic properties in a magnetic storage material often requires the build-up of rather complex film structures and multilayers containing alloys or compounds. This usually involves a larger number of different chemical species. In parallel with the system's chemical complexity, there is a growing need to characterize the magnetic contribution of its individual chemical components. The discovery of X-ray magnetic circular dichroism (MCD) [6] marked an important advance in the development of appropriate analytical procedures [7].

One of the major challenges brought about by such complex systems is the elementally resolved imaging of their magnetic microstructures. Several well-established techniques for magnetic domain imaging are available, such as Kerr microscopy [8,9], scanning electron microscopy with spin polarization analysis (SEMPA) [10], or Lorentz microscopy [11,12], to name but a few. Each of these approaches has its specific virtues and drawbacks.

The diffraction-limited spatial resolution in Kerr microscopy is insufficient for the investigation of new generation storage media with lateral bit dimensions significantly below 1 μm . Electron beam based methods with their higher lateral resolution are better suited for this purpose. SEMPA, however, is inherently surface sensitive, and thus it is not very well adapted to the analysis of buried layers. Finally, Lorentz microscopy is a transmission electron microscopy technique and can be used only for very thin samples. Common to all of the above techniques, however, is their lack of ability to separate the magnetic contributions from the various chemical species in a complex thin film structure.

2. Contrast mechanisms and instrumentation

Recent observations of magnetic dichroism in the emission characteristics of core level photoelectrons and in photoinduced secondary electron yield open up entirely new possibilities for magnetic domain imaging. Irradiating a homogeneously magnetized sample with circularly or linearly polarized soft X-rays, one observes a clear variation in the intensity of the photoelectrons or secondary electrons upon magnetization reversal. This technique is already used in a number of spectroscopies, where it often replaces explicitly spin-resolving approaches. If the same approach is introduced into a microscopy technique, an image taken from a magnetic surface containing several domains will show a modulation of the laterally resolved photocurrent associated with the local orientation of the magnetization, i.e. the domain pattern. This magnetic contribution can then be separated by suitable image processing.

The various magneto-dichroic effects which have been reported so far fall into two classes. The first type of magnetic dichroism is found at adsorption edges. These effects include circular magnetic dichroism (CMD) in the total electron yield [13], CMD in Auger electron emission

* Fax: +49-345-551-1223.

[14], and linear magnetic dichroism (LMD) in the total yield [15]. The latter may be seen as a direct high-energy counterpart to the familiar transverse magneto-optic Kerr effect. All of these phenomena are associated with the unoccupied spin-split density of states below the vacuum level and are therefore bound to characteristic excitation energies. At photon energies exceeding the absorption edges we find magneto-dichroic phenomena in the electron emission characteristics, so-called magnetic dichroism in the angular distribution of photoelectrons (MDAD). MDAD is associated with the exchange induced spin-splitting in the core states and has been observed with circularly polarized (CMDAD) [16], linearly polarized (LMDAD) [17,18], and even unpolarized light (UMDAD) [19]. Due to their different physical origins, MD and MDAD phenomena differ in their angular dependencies. The absolute magnitude of a magnetic dichroism in total or partial yield depends only on the angle between the magnetization and the photon spin (or equivalently, the photon wave vector). In contrast, the sign and magnitude of a magnetic dichroism in the angular distribution is distinctly determined by the wave vector of the emitted electron, too. Observation of MDAD effects therefore requires appropriate angular resolution. These angular dependencies connect each form of magnetic dichroism to a particular geometry, in which the maximum dichroic signal can be observed. Both classes of magnetic dichroism can in principle be used for magnetic imaging purposes, if an appropriate electron-optical column and a suitable experimental geometry are chosen.

The magnetic information depth is determined by the inelastic mean free path of the electrons.

An experiment for the imaging of magnetic microstructures by means of magnetic dichroism can draw on the wealth of experience gained in the field of chemically selective imaging of surfaces. In particular, parallel imaging techniques are of interest here. Two approaches have already been successfully employed in magneto-dichroic domain imaging: the photoelectron emission microscope (PEEM) [20] and imaging electron spectrometers [14,21]. These two types of instruments involve nearly diametrically different electron-optical concepts. A photoemission microscope based on the immersion lens concept (PEEM) collects almost all electrons emitted from the sample due to the strong acceleration potentials. Because of this angular integration, the magnetic contrast can only arise from MCD in the total electron yield. The low transmission of the instrument for high-energy electrons, however, finally results in an effective low-pass behavior. The image is thus generated predominantly by the low-energy secondary electrons. In order to reduce further the energy spread of the electrons, contemporary versions of the PEEM employ an additional energy filter. The electron-optics of an imaging electron spectrometer, however, is clearly constructed with an emphasis on the spectroscopy aspect, i.e. with a high transmission over a broad range of kinetic energies. Such an instrument is therefore predestined to access magnetic dichroism in the emission of electrons at higher kinetic energies, e.g. Auger electrons and core level photo-

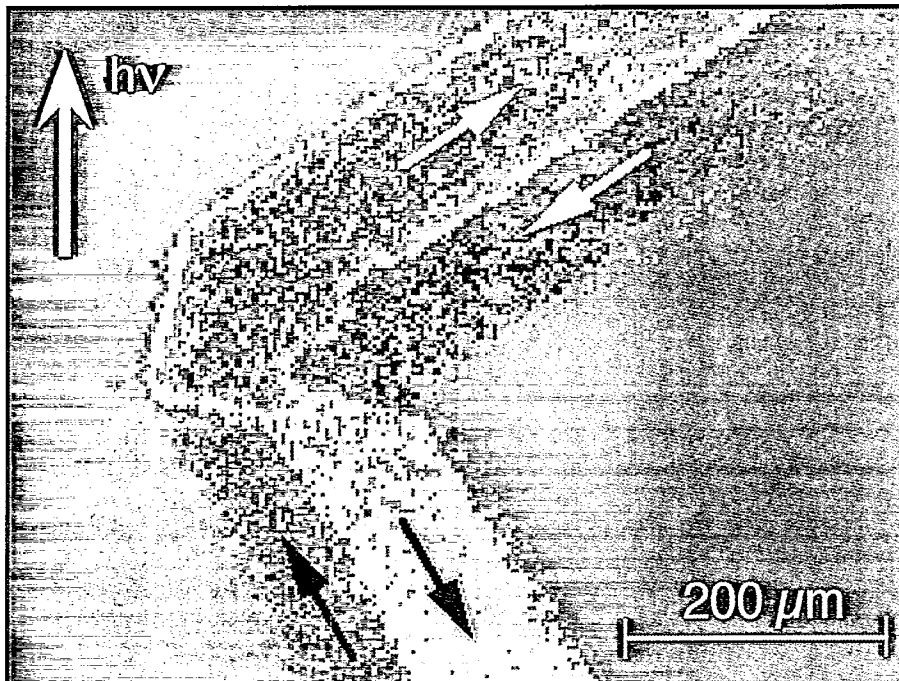


Fig. 1. Magnetic domain pattern of an Fe(100) whisker surface obtained by spectro-microscopy using magnetic circular dichroism in the emission of Fe Auger electrons. The arrows give the orientations of the local magnetization in the individual domains.

electrons (a high kinetic energy may even allow imaging under weak applied magnetic fields). In addition, only electrons emitted into a small solid angle are used to form the image. The technique can therefore exploit both MD and MDAD effects as contrast mechanisms [22]. A drawback of imaging electron spectrometers is their presently rather moderate spatial resolution of $\sim 1 \mu\text{m}$, whereas PEEM-type instruments routinely achieve values well below $1 \mu\text{m}$.

3. Selected results

An example of magnetic domain imaging with an imaging electron spectrometer is given in Fig. 1. The sample was an L-shaped Fe(100) whisker mounted on a Mo plate. Only LMV Auger electrons from iron with a kinetic energy of 648 eV have been selected to form the image. The direction of incidence of the circularly polarized light made an angle of 25° with the whisker surface. The magnetic contrast arises from the magnetic circular dichroism at the Fe $L_{2,3}$ absorption edges [21]. Since the magneto-dichroic signals at the L_2 and L_3 edges are of approximately the same absolute value, but of opposite sign, the following procedure is used to separate the magnetic information. In a first step, an image is taken at each edge, $L_2(x, y)$ and $L_3(x, y)$. In the second step, an asymmetry image $A(x, y)$ is calculated according to

$$A(x, y) = [L_2(x, y) - L_3(x, y)] / [L_2(x, y) + L_3(x, y)], \quad (1)$$

in close analogy with the determination of the intensity asymmetry or magneto-dichroic signal in an electron spectroscopy experiment. In the resulting image $A(x, y)$ other contrast mechanisms, such as chemical or topography contrasts, have been effectively eliminated.

The resulting domain pattern in Fig. 1 exhibits four different spatial orientations of the magnetization, as expected from a fourfold symmetric surface. In general, MCD is sensitive only to the component of the local magnetization vector \mathbf{M} parallel to the direction of incidence, or equivalently, to the photon spin σ , i.e. the dichroic signal behaves as

$$A \propto \sigma \cdot \mathbf{M}. \quad (2)$$

In Fig. 1 the whisker has been rotated in such a way that the magnetizations in all four domains have different projections along the photon wave vector (or equivalently, photon spin), thus giving rise to four distinctly different gray levels. This 'vectorial' imaging is facilitated by the fact that the magneto-dichroic signal for iron is rather large (about 30% peak-to-peak). The domain pattern in Fig. 1 shows the almost ideal case for this particular shape of the Fe(100) whisker. On each leg of the 'L', one finds only two large domains separated by a 180° domain wall. In the

elbow region of the 'L' the domains are bounded by 90° walls. This example demonstrates the general applicability of magnetic dichroism for magnetic domain imaging.

The contrast mechanism employed to obtain Fig. 1 is directly associated with the magnetic circular dichroism in the $L_{2,3}$ absorption. The absorption process generates a 2p core hole which subsequently decays via Auger transitions. The dichroism in the absorption is therefore also reflected in the Auger electron yield. Since the Auger electrons have the highest kinetic energy in the spectrum of the emitted electrons, they are practically background-free. Exciting at a specific absorption edge and accepting only the corresponding Auger electrons one gains an extreme chemical sensitivity. These Auger electrons, however, undergo inelastic scattering processes and are thus the starting point for a secondary electron cascade, which also contains a magneto-dichroic signal. A PEEM forms an image with the low-energy part of this secondary electron cascade. This technique has been successfully employed to image written domains in a magnetic storage material [20]. Depending on the specific situation, the low-energy secondary electron yield generally contains some 'non-dichroic' background, for example, due to the excitation of core levels at lower binding energies and the associated Auger transitions. This contribution may reduce the maximum achievable contrast as compared with the Auger electron yield, causing some difficulties if very low contrast levels are involved.

An example of the kind of information obtained with the element specificity of this method is given in Fig. 2, which compares the domain pattern on the clean whisker surface with that of one monolayer of chromium on the iron surface. Fig. 2(a) shows a slightly different part of the whisker in Fig. 1, where only two oppositely magnetized domains are visible. In addition, the whisker has been rotated to maximize the component of local magnetization along the photon spin. The contrast achieved in this way is depicted in the inset as a line scan perpendicular to the domain wall and reaches a peak-to-peak value of about 30%. After deposition of a monolayer of chromium, a domain pattern was recorded using Cr LMV Auger electrons with a kinetic energy of 529 eV. The photon energy was adjusted to the respective Cr $L_{2,3}$ absorption lines. By means of this procedure, exclusively the magnetic response of the chromium monolayer is probed. The resulting image (Fig. 2b) has an inferior signal-to-noise ratio (essentially determined by the counting statistics and the small signal from a single layer) and shows a weak, but discernible contrast. The vertical line scan reveals a peak-to-peak asymmetry of about 3%. Comparing Fig. 2(a) and (b), it becomes obvious that the domain contrast in the Cr overlayer is reversed. This indicates that the local magnetization in the Cr film is aligned antiparallel to that of the iron substrate. Further investigations of the Fe signal prove that the domain structure of the whisker surface is unaffected by the presence of the chromium film. These results lead

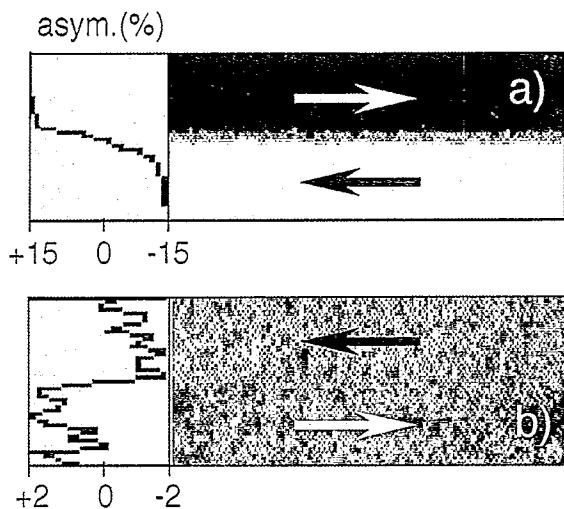


Fig. 2. (a) Magnetic domain pattern of a clean Fe(100) whisker surface recorded with Fe LMV Auger electrons. The image shows a region with a single 180° wall (inset: vertical line scan showing the contrast between the two oppositely magnetized domains). (b) Magnetic domain pattern in a chromium monolayer deposited onto the iron surface in (a). This image was obtained with Cr LMV Auger electrons ($E_{\text{kin}} = 529$ eV) and excitation at the Cr $L_{2,3}$ edge (inset: vertical line scan showing the contrast reversal due to the antiferromagnetic coupling of the Cr overlayer to the Fe substrate).

unambiguously to the conclusion that the chromium overlayer couples antiferromagnetically to the iron substrate.

The magneto-dichroic signal from the Cr film disappears quickly with increasing film thickness. Films of 3 ML thickness do not exhibit any domain contrast above the noise level. This supports the model of topological antiferromagnetism for Cr(001). Seen along the (001) direction neighboring planes are oppositely magnetized, causing the dichroic signals from neighboring layers to cancel each other. The total magnetic dichroism from a stack of Cr layers will thus be close to zero. If, in addition, the film is subject to a certain roughness, this cancellation may be even more effective. Taking into account the film roughness could explain the small magneto-dichroic signal observed for the chromium monolayer (Fig. 2b, inset). In comparison with an ideal flat monolayer, a film containing a sizable fraction of bilayer islands will exhibit a reduced magneto-dichroic signal, because the topological antiferromagnetism reduces significantly the contribution from the bilayer islands. The result for the Cr monolayer nicely demonstrates the current sensitivity limit of the method. In the case of ferromagnetic overlayers, the magnetic microstructure could be imaged even in the submonolayer regime.

4. Outlook

Investigations of magnetic microstructures by means of magneto-dichroic effects are only just beginning. The main

virtue of this approach is the combination of magnetic sensitivity with elemental selectivity. This makes the approach uniquely suited to investigations of magnetic phenomena in complex thin film systems which are of interest for technical applications. Electron emission microscopies based on magneto-dichroic phenomena with circularly and linearly polarized light are likely to become versatile tools in the characterization of magnetic materials.

To date these approaches suffer from two major limitations. First, the spatial resolution of the available instruments is relatively poor ($10 \mu\text{m}$ in the case of the above spectro-microscopy approach, and about $1 \mu\text{m}$ in the first magneto-dichroic PEEM experiments [20]). Second, the acquisition times are comparably long, in particular for spectro-microscopy experiments, since these select only a small fraction of the photocurrent. Some of these limitations, however, will soon be surpassed by the development of suitable electron-optical imaging systems. For a PEEM with an integrated energy filter, a spatial resolution of about 40 nm in synchrotron radiation experiments has already been reported very recently [23]. The access to dedicated beamlines and high brilliance synchrotron radiation sources of the next generation will lead to a further reduction in the acquisition times and may even permit quasi-dynamic investigations in selected systems.

In future applications of these techniques basically all types of magnetic dichroism may be utilized as possible contrast mechanisms. These include the various types of magneto-dichroic effects in the emission of core level photoelectrons [14,17,18,21,22], which are also highly element-specific. Of particular interest will be the exploitation of magneto-dichroic effects observed with linearly polarized synchrotron radiation. Linearly polarized synchrotron radiation with high brilliance is currently more readily available. Magneto-dichroic effects in the emitted photoelectrons can in principle also be observed with unpolarized radiation generated in conventional laboratory X-ray tubes [19]. Because of reasons of brilliance, however, the exploitation of the unpolarized magnetic dichroism with laboratory sources will probably be limited to spectroscopy applications.

Acknowledgement: The author gratefully acknowledges a fruitful collaboration with J. Kirschner, K. Meinel, M. Neuber and M. Grunze. Special thanks go to B. Heinrich and Z. Celinski for helpful discussions and the iron whiskers. The work was supported by the Bundesministerium für Forschung und Technologie (grants No. 055EFAAI5 and No. 055VHFx1).

References

- [1] P. Grünberg, R. Schreiber, Y. Pang, M.B. Brodsky and H. Sowers, Phys. Rev. Lett. 64 (1986) 2442.
- [2] S.S.P. Parkin, N. More and K.P. Roche, Phys. Rev. Lett. 64 (1990) 2304.
- [3] J. Unguris, R.J. Celotta and D.T. Pierce, Phys. Rev. Lett. 67 (1991) 140.

- [4] M.N. Baibich, J.M. Broto, A. Fert, F. Nguyen Van Dau, F. Petroff, P. Etienne, G. Creuzet, A. Friederich and J. Chazelas, *Phys. Rev. Lett.* 61 (1988) 2472.
- [5] G. Binasch, P. Grünberg, F. Saurenbach and W. Zinn, *Phys. Rev. B* 39 (1989) 4828.
- [6] G. Schütz, W. Wagner, W. Wilhelm, P. Kienle, R. Zeller, R. Frahm and G. Materlik, *Phys. Rev. Lett.* 58 (1987) 737.
- [7] C.T. Chen, Y.U. Idzerda, H.-J. Lin, G. Meigs, A. Chaiken, G.A. Prinz and G.H. Ho, *Phys. Rev. B* 48 (1993) 642.
- [8] J. Kranz and A. Hubert, *Z. Angew. Phys.* 15 (1963) 220.
- [9] F. Schmidt, W. Rave and A. Hubert, *IEEE Trans. Magn.* 21 (1985) 1596.
- [10] H.P. Oepen and J. Kirschner, *Scanning Microsc.* 5 (1991) 1.
- [11] E. Fuchs, *Naturwiss.* 47 (1960) 392.
- [12] J.N. Chapman, *J. Phys. D* 17 (1984) 623.
- [13] C.T. Chen, F. Sette, Y. Ma and S. Modesti, *Phys. Rev. B* 42 (1990) 7262.
- [14] C.M. Schneider, K. Meinel, K. Holldack, H.P. Oepen, M. Grunze and J. Kirschner, *Mater. Res. Soc. Symp. Proc.* 313 (1993) 631.
- [15] F.U. Hillebrecht, private communication.
- [16] C.M. Schneider, D. Venus and J. Kirschner, in: *Vacuum Ultraviolet Radiation Physics*, eds. F.J. Wuilleumier, Y. Petroff and I. Nenner (World Scientific, Singapore, 1992), p. 421.
- [17] C. Roth, F.U. Hillebrecht, H.B. Rose and E. Kisker, *Phys. Rev. Lett.* 70 (1993) 3479.
- [18] C. Roth, H.B. Rose, F.U. Hillebrecht and E. Kisker, *Solid State Commun.* 86 (1993) 647.
- [19] F.U. Hillebrecht and W.-D. Herberg, *Z. Phys. B: Condens. Matter* 93 (1994) 299.
- [20] J. Stöhr, Y. Wu, M.G. Sarmant, B.D. Hermsmeier, G. Harp, S. Koranda, D. Dunham and B.P. Tonner, *Science* 259 (1993) 658.
- [21] C.M. Schneider, K. Holldack, M. Kinzler, M. Grunze, H.P. Oepen, F. Schäfers, H. Petersen, K. Meinel and J. Kirschner, *Appl. Phys. Lett.* 63 (1993) 2432.
- [22] C.M. Schneider, Z. Celinski, M. Neuber, C. Wilde, M. Grunze, K. Meinel and J. Kirschner, *J. Phys.: Condens. Matter* 6 (1994) 1177.
- [23] G. Lilienkamp, private communication.